THE JOURNAL OF BIOLOGICAL CHEMISTRY VOL. 283, NO. 39, pp. 26726–26736, September 26, 2008

Phosphorylation of HsMis13 by Aurora B Kinase Is Essential for Assembly of Functional Kinetochore*[S]

Received for publication, June 2, 2008, and in revised form, July 15, 2008 Published, JBC Papers in Press, July 17, 2008, DOI 10.1074/jbc.M804207200

Yong Yang[‡§], Fang Wu[‡], Tarsha Ward[§], Feng Yan[‡§], Quan Wu[‡§], Zhaoyang Wang[‡], Tanisha McGlothen[§], Wei Peng[¶], Tianpa You[‡], Mingkuan Sun[‖§], Taixing Cui[‡], Renming Hu[**], Zhen Dou[‡§], Jingde Zhu[‡], Wei Xie[‖], Zihe Rao[¶], Xia Ding[§‡‡1], and Xuebiao Yao[‡2]

From the [‡]Hefei National Laboratory for Physical Sciences at Micro-scale and University of Science and Technology of China, Hefei 230027, China, [**]Department of Endocrinology and Metabolism, Huashan Hospital, Fudan University, Shanghai 200040, China, [‖]MOE Key Laboratory of Developmental Genes and Human Disease, Southeast University Medical School, Nanjing 210009, China, [‖]Department of Medicine, Beijing University of Chinese Medicine, Beijing 100029, China, [¶]Institute of Biophysics, Chinese Academy of Sciences, Beijing 100101, China, and [§]Cancer Biology Program, Morehouse School of Medicine, Atlanta, Georgia 30310

Chromosome movements in mitosis are orchestrated by dynamic interactions between spindle microtubules and the kinetochore, a multiprotein complex assembled onto centromeric DNA of the chromosome. Here we show that phosphorylation of human HsMis13 by Aurora B kinase is required for functional kinetochore assembly in HeLa cells. Aurora B interacts with HsMis13 *in vitro* and *in vivo*. HsMis13 is a cognate substrate of Aurora B, and the phosphorylation sites were mapped to Ser-100 and Ser-109. Suppression of Aurora B kinase by either small interfering RNA or chemical inhibitors abrogates the localization of HsMis13 but not HsMis12 to the kinetochore. In addition, non-phosphorylatable but not wild type and phospho-mimicking HsMis13 failed to localize to the kinetochore, demonstrating the requirement of phosphorylation by Aurora B for the assembly of HsMis13 to kinetochore. In fact, localization of HsMis13 to the kinetochore is spatiotemporally regulated by Aurora B kinase, which is essential for recruiting outer kinetochore components such as Ndc80 components and CENP-E for functional kinetochore assembly. Importantly, phospho-mimicking mutant HsMis13 restores the assembly of CENP-E to the kinetochore, and tension developed across the sister kinetochores in Aurora B-inhibited cells. Thus, we reason that HsMis13 phosphorylation by Aurora B is required for organizing a stable bi-oriented microtubule kinetochore attachment that is essential for faithful chromosome segregation in mitosis.

The kinetochore is a super-molecular complex assembled at each centromere in eukaryotes. It provides a chromosomal attachment point for the mitotic spindle, linking the chromosome to the microtubules and functions in initiating, controlling, and monitoring the movements of chromosomes during mitosis. The kinetochore of animal cells contains two functional domains; that is, the inner kinetochore, which is tightly and persistently associated with centromeric DNA sequences throughout the cell cycle and the outer kinetochore which is composed of many dynamic protein complexes that interact with microtubules only during mitosis. The stable propagation of eukaryotic cells requires each chromosome to be accurately duplicated and faithfully segregated. During mitosis, attaching, positioning, and bi-orientating kinetochores with the spindle microtubules play critical roles in chromosome segregation and genomic stability (see Refs. 1 and 2).

Mitosis is orchestrated by signaling cascades that coordinate mitotic processes and ensure accurate chromosome segregation. The key switch for the onset of mitosis is the archetypal cyclin-dependent kinase Cdk1. In addition to the master mitotic kinase Cdk1, three other protein serine/threonine kinase families are also involved, including the Polo kinases, Aurora kinases, and the NEK[3] (NIMA-related kinases) (*e.g.* Refs. 3 and 4). Recent studies have demonstrated the involvement of NEK kinase in stabilization of the kinetochore-microtubule attachment (*e.g.* Ref. 5) and the critical role of Aurora B kinase in kinetochore bi-orientation (*e.g.* Ref. 6). Whereas the mechanism ensuring chromosome bi-orientation lies at the heart of chromosome segregation control, the molecular details remain elusive.

Early studies to isolate temperature-sensitive fission yeast mutants that displayed high loss rates of mini-chromosomes at permissive or semi-permissive temperatures led Yanagida and co-workers (7) to identify 12 genetic loci (Mis1–12). Their subsequent studies show that centromere proteins Mis12 and Mis6 determine the proper metaphase spindle length and are required for faithful chromosome segregation in yeast (*e.g.* Ref.

* This work was supported, in whole or in part, by National Institutes of Health Grants DK56292, CA132389, and CA92080. This work was also supported by grants from Chinese 973 Project (2002CB713700, 2006CB943603, and 2007CB914503), Chinese Academy of Sciences (KSCX1-YW-R65 and KSCX2-YW-H10), Chinese 863 Project (2006AA02A247), Chinese Ministry of Education (20020358051 and 20050358061 and 111 Project B07007 (to X. D.), Chinese Natural Science Foundation (90508002 and 30121001 (to X. Y.), 30500183 (to X. D.), and 30600321 (to Z. D.)), American Cancer Society (RPG 99-173-1), and an Atlanta Clinical and Translational Science Award Chemical Biology grant (to X. Y.). The costs of publication of this article were defrayed in part by the payment of page charges. This article must therefore be hereby marked "*advertisement*" in accordance with 18 U.S.C. Section 1734 solely to indicate this fact.

[S] The on-line version of this article (available at http://www.jbc.org) contains supplemental Fig. S1.

[1] To whom correspondence may be addressed. E-mail: xding@bucm.edu.cn.

[2] A Georgia Cancer Coalition Eminent Cancer Research Scholar. To whom correspondence may be addressed. E-mail: yaoxb@ustc.edu.cn.

[3] The abbreviations used are: NEK, NIMA-related kinase; PBS, phosphate-buffered saline; GFP, green fluorescent protein; GST, glutathione *S*-transferase; siRNA, small inhibitory RNA; DAPI, 4′,6-diamidino-2-phenylindole; PIPES, 1,4-piperazinediethanesulfonic acid.

8). Initial studies of the Mis12 orthologue in human cells suggest that it is required for proper chromosome alignment and segregation (9). Recent studies show that the Mis12 complex contains four components (Mis12, Dsn1, Nsl1, and Nnf1), which are conserved from yeast to human (Refs. 10–12; for clarity we referred them as HsMis12, HsMis13, HsMis14, and HsMis15, respectively). These four proteins function at the inner kinetochores are required for proper chromosome alignment and chromosome segregation in mitosis (13). However, the molecular mechanisms underlying Mis12 complex assembly to the kinetochore and the regulation of its association with other kinetochore complexes such as Ndc80 remained elusive.

Recent studies suggest a critical role for Aurora B in kinetochore bi-orientation and aberrant kinetochore-microtubule attachment correction. To delineate the regulatory function of Aurora B in kinetochore protein-protein interactions, we adopted a quick search for Aurora B-binding proteins using a "high content" Far Western assay that had successfully identified NEK2A-Sgo1 and NEK2A-Hec1 interactions (5, 14). This approach led to the identification of an interrelationship between Aurora B and HsMis13. Our biochemical characterization demonstrated that HsMis13 is a novel substrate of Aurora B. Most importantly, the phosphorylation of HsMis13 by Aurora B is essential for assembly of functional kinetochore. We propose that Aurora B-mediated phosphorylation of HsMis13 provides a regulatory mechanism underlying kinetochore assembly and bi-orientation essential for faithful chromosome segregation in mitosis.

MATERIALS AND METHODS

Cell Culture and Synchronization—HeLa and 293T cells from American Type Culture Collection (Manassas, VA) were maintained as subconfluent monolayers in DMEM (Invitrogen) with 10% fetal bovine serum (Hyclone, Logan, UT) and 100 units/ml penicillin plus 100 μg/ml streptomycin (Invitrogen) at 37 °C with 10% CO_2. Cells were synchronized at G_1/S with 2 mM thymidine for 16 h, then washed with phosphate-buffered saline (PBS) three times and cultured in thymidine-free medium for 12 h to release. After another round of thymidine treatment for 12 h, cells were released for 9 h to reach prometaphase and 11 h to synchronize at telophase. In some cases 100 nM nocodazole was added to cell culture for 18 h to synchronize cells in prometaphase.

cDNA Construction—To generate GFP-tagged full-length HsMis13, PCR-amplified HsMis13 cDNA was digested with BgLII and SalI and then cloned into pEGFP-C3 vector (Clontech). The bacterial expression constructs of HsMis13 were cloned into pGEX-6P-1 vector (Amersham Biosciences) with SmaI digestion. FLAG-tagged HsMis13 cDNA was cloned by inserting the PCR product into the p3XFLAG-*myc*-CMV-24 vector (Sigma) with EcoRV digestion. GFP-tagged non-phosphorylatable and phosphormimetic HsMis13 mutants were created by standard PCR methods as described previously (*e.g.* Ref. 15). All constructs were sequenced in full.

Recombinant Protein Expression—Human HsMis13 was expressed in bacteria as a GST fusion protein. Briefly, 500 ml of LB media was inoculated with bacteria Rosetta (DE3) pLysS transformed with GST-HsMis13. The protein expression was initiated by the addition of 0.2 mM isopropyl 1-thio-β-D-galactopyranoside and incubation at 16 °C for 12 h. Bacteria were then collected by centrifugation and resuspended in PBS containing a protease inhibitor mixture (Sigma) followed by sonication and clarification. The GST fusion protein in bacteria in the soluble fraction was purified by using glutathione-agarose chromatography according to the manufacturer's protocol.

Antibodies—Affinity purification of CENP-E rabbit antibody was described previously (16). Mouse monoclonal antibody to Nuf2 was purchased from Abcam and diluted at 1:1000 for Western blot and 1:300 for immunofluorescence. Mouse monoclonal antibody to Hec1 was purchased from Abcam and diluted at 1:1000 for Western blot and 1:500 for immunofluorescence. Mouse monoclonal antibodies to GST was purchased from Cell Signaling (Beverly, MA) and used at a 1:1000 dilution for Western blot. Mouse monoclonal antibody to GFP was obtained from BD Biosciences.

Purified His-HsMis13 from inclusion body was used to immunize rabbit and Balb/C mice according to the general protocol. The purified IgG was obtained by affinity purification using an HsMis13 affinity matrix based on CNBr-activated agarose beads (Sigma).

Immunoprecipitation—Co-immunoprecipitation was performed as described previously (*e.g.* Ref. 17). Briefly, 293T cells growing on 100-mm Petri dishes were transfected with appropriate plasmids for 36 h. Cells were lysed in lysis buffer (50 mM Tris, pH 6.8, 150 mM NaCl, 2 mM EGTA, 0.1% Triton X-100, 1 mM $MgCl_2$, 1 mM phenylmethanesulfonyl fluoride, and protease inhibitors). After centrifugation, the supernatant was incubated with 25 μl of 50% slurry of anti-FLAG M2 affinity resin (Sigma) for 4 h at 4 °C. After washing 3 times in cold lysis buffer, the beads were boiled in 50 μl of SDS sample buffer. For immunoblotting, mouse monoclonal anti-GFP antibody was diluted 1:2000 and anti-FLAG M2 monoclonal (Sigma) was diluted to 3 μg/ml.

In some instances HeLa cells were synchronized at prophase and telophase as described above. The cells were then lysed using lysis buffer (0.5% Nonidet P-40, 50 mM Tris-Cl, pH 7.4, 150 mM NaCl, 5 mM EDTA, 0.02% sodium azide, 1 mM phenylmethanesulfonyl fluoride was added before use). HsMis13 antibody was incubated with protein A/G beads. Protein-bound protein A/G beads were washed 3 times by wash buffer (0.1% Nonidet P-40, 50 mM Tris-Cl, pH 7.4, 150 mM NaCl, 5 mM EDTA, 0.02% sodium azide, phenylmethanesulfonyl fluoride was added just before use) to prepare for the immunoprecipitation experiment. These antibody-bound A/G beads were added to cell lysate and incubated for 4 h at 4 °C. After incubation, beads were washed four times with wash buffer and once with PBS. Samples were resolved by 10% SDS-PAGE and transferred onto nitrocellulose membrane to perform Western blot.

For immunoprecipitation of transiently transfected cells, HeLa cells were generally collected 42 h after transfection of GFP-HsMis13 and GFP-HsMis13^{AA}, which included an 18-h nocodazole synchronization. Cellular proteins were solubilized in lysis buffer and clarified by centrifugation. GFP-HsMis13 proteins were precipitated using a rabbit anti-GFP antibody bound to protein-A/G beads (Pierce). Beads were washed five times with lysis buffer and then boiled in protein sample buffer

for 2 min. After SDS-PAGE, proteins were transferred to nitrocellulose membrane. The membrane was probed with antibodies against GFP and phospho-serine (Sigma) as described (5).

Transfection and Immunofluorescence—Cells were transfected with small inhibitory RNA (siRNA)- or GFP-tagged plasmids in a 24-well plate by Oligofectamine reagent and Lipofectamine 2000 (Invitrogen), respectively, according to the manufacture's manuals.

For immunofluorescence, HeLa cells were seeded onto sterile, acid-treated 12-mm coverslips in 24-well plates (Corning Glass Works, Corning, New York). Double thymidine-blocked and -released HeLa cells were transfected with 1 μl of Lipofectamine 2000 premixed with 1 μg of various plasmids as described above. In general, 36–48 h after transfection, HeLa cells were rinsed for 1 min with PHEM buffer (100 mM PIPES, 20 mM HEPES, pH 6.9, 5 mM EGTA, 2 mM $MgCl_2$, and 4 M glycerol) and permeabilized for 1 min with PHEM plus 0.1% Triton X-100. Extracted cells were then fixed in freshly prepared 4% paraformaldehyde in PHEM and rinsed three times in PBS. Cells on the coverslips were blocked with 0.05% Tween 20 in PBS (TPBS) with 1% bovine serum albumin (Sigma). These cells were incubated with various primary antibodies in a humidified chamber for 1 h and then washed three times in TPBS. Primary antibodies were visualized using fluorescein isothiocyanate-conjugated goat anti-mouse IgG or rhodamine-conjugated goat anti-rabbit IgG. DNA was stained with 4′,6-diamidino-2-phenylindole (Sigma).

Antibodies against HpX, GFP, Nuf2, Hec1, ACA, HsMis12, and HsMis13 were used at the dilution of 1:500, 1:300, 1:300, 1:500, 1:500, 1:100, and 1:100, respectively. Images were acquired using an Axiovert200 inverted Microscope (Carl Zeiss) with Axiovision 3.0 software.

In Vitro Kinase Assay—His-tagged Aurora B kinase was expressed in bacteria and purified by nickel-nitrilotriacetic acid beads. The kinase reactions were performed in 40 μl of 1× kinase buffer (25 mM HEPES, pH 7.2, 5 mM $MgSO_4$, 1 mM dithiothreitol, 50 mM NaCl, 2 mM EGTA) containing 1 μl of eluted Aurora B kinase, 5 μl of glutathione bead-bound GST-Mis13, 5 μCi of [γ-^{32}P]ATP, and 50 μM ATP. The mixtures were incubated at 30 °C for 30 min. The reactions were stopped with 2× SDS sample buffer and separated by SDS-PAGE. The gel was stained with Coomassie Brilliant Blue and dried, and the ^{32}P incorporation into HsMis13 proteins was quantified by a PhosphorImager (Amersham Biosciences). The specific incorporation of ^{32}P into wild type HsMis13 and non-phosphorylatable $HsMis13^{S100A/S109A}$ was normalized to protein levels and expressed as relative activity to the wild type protein.

siRNA—For the siRNA studies, the 21-mer of siRNA duplexes against HsMis13 and Aurora B were synthesized by Dharmacon Research Inc. (Lafayette, CO) as previously described (11, 13, 18). As a control, either a duplex targeting cyclophilin or scramble sequence was used (11).

The transfection efficiency was judged based on the uptake of the fluorescein isothiocyanate-conjugated oligonucleotides, whereas the efficiency of siRNA-mediated protein suppression was judged by Western blotting analysis (*e.g.* Ref. 11). After trial experiments using a series of concentration and time course assay, treatment of 150 nM for 36 h was finally selected as the most efficient conditions for repressing target proteins.

Fluorescence Intensity Quantification and Kinetochore Distance Measurement—Fluorescence intensity of kinetochore protein labeling was measured by using the confocal microscope LSM510 NLO (Carl Zeiss) scan head mounted transversely to an inverted microscope (Axiovert 200; Carl Zeiss) with a 100 × 1.3 NA PlanApo objective. The images from double labeling were collected using a dichroic filter set with Zeiss image processing software (LSM 5, Carl Zeiss). The distance between sister kinetochores marked with ACA was measured as the distance between the peak fluorescence as previously described (17).

The quantification of the level of kinetochore-associated protein was conducted as described by Johnson *et al.*, (18) and more recently by Liu *et al.* (24). In brief, the average pixel intensities from at least 100 kinetochore pairs from five cells were measured, and background pixel intensities were subtracted. The pixel intensities at each kinetochore pair were then normalized against ACA pixel values to account for any variations in staining or image acquisition. The values of specific siRNA-treated cells were then plotted as a percentage of the values obtained from cells transfected with a control siRNA duplex.

RESULTS

HsMis13 Is a Novel Aurora B Binding Partner—To delineate the molecular mechanism underlying Aurora B regulation in kinetochore protein-protein interaction networks, we immobilized bacterially recombinant kinetochore proteins onto a nitrocellulous membrane to conduct a quick search for Aurora B-binding proteins using a high content Far Western assay (5, 14). The Aurora B binding activity was then detected by an anti-Aurora B monoclonal antibody. One advantage of such a high-content assay is to screen a large number of potential interacting proteins in parallel yet avoid initial intensive labor spent on purifying large quantities of proteins required for pull-down assays. This assay has detected the binding activity of several known Aurora B-interacting proteins, such as Hec1, validating the sensitivity of such an assay (supplemental Fig. 1). This assay is very specific, as Aurora B was never found to be associated with GST tag, maltose-binding protein tag, or bovine serum albumin. Interestingly, Aurora B was found to associate with HsMis13 immobilized onto the membrane (supplemental Fig. 1, *C1*), suggesting a potential interaction between Aurora B kinase and HsMis13 protein.

To examine whether HsMis13 forms a cognate complex with Aurora B in cells, we carried out an immunoprecipitation using mitotic lysates from 293T cells transiently transfected to express FLAG-HsMis13 and GFP-Aurora B (both wild type and kinase death mutant). As shown in Fig. 1*A*, Western blot using GFP antibody confirmed that Aurora B was pulled down by FLAG-HsMis13 (*lanes 5* and *6*; *upper blot*). However, a greater amount of wild type Aurora B was recovered in FLAG-HsMis13 immunoprecipitates compared with that of kinase-death Aurora B mutant. No GFP tag was precipitated with FLAG-HsMis13 (*lane 4*). Thus, we conclude that HsMis13 interacts with Aurora B *in vivo*.

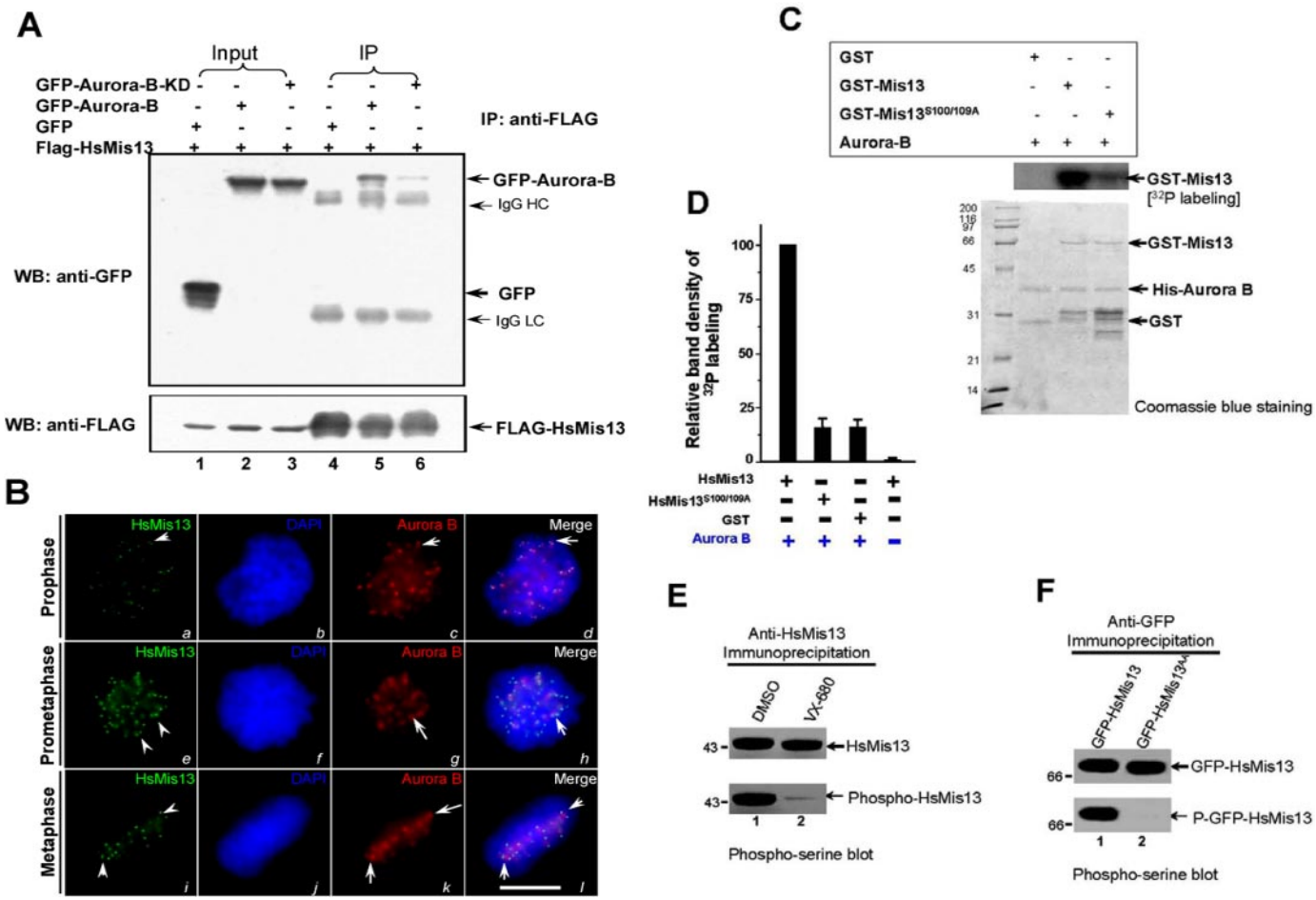

FIGURE 1. **Aurora B interacts with HsMis13 *in vitro* and *in vivo*.** *A*, co-immunoprecipitation of HsMis13 and GFP-Aurora B from 293T cells. Extracts from cells transiently transfected to express GFP-Aurora B (both wild type and kinase-death mutant) and FLAG-HsMis13 or GFP and FLAG-HsMis13 were incubated with antibodies against FLAG (*lanes 4–6*), and immunoprecipitates (*IP*) were resolved by SDS-PAGE. *Lane 4*, immunoprecipitation from GFP-and-FLAG-HsMis13-transfected cell extracts. Western blotting (*WB*) verified co-immunoprecipitation of Aurora B (*upper panel*; GFP blot) and HsMis13 (*lower panel*). Note that FLAG-HsMis13 preferentially pulled down wild type but not kinase-death Aurora B. *HC*, heavy chain; *LC*, light chain. *B*, co-distribution of HsMis13 with Aurora B in dividing cells. Asynchronized HeLa cells were stained with HsMis13 rabbit antibody, Aurora B mouse antibody, and DAPI. Note that HsMis13 appeared as pairs of separate *double dots* from prophase to metaphase. The *scale bar* represents 10 μm. *C*, Ser-100 and Ser-109 of HsMis13 are substrates of Aurora B. Bacterially expressed GST-HsMis13 fusion proteins, both wild type and mutant (S100A/S109A), were purified and phosphorylated *in vitro* using [^{32}P]ATP and active Aurora B as described under "Materials and Methods." Samples were separated by SDS-PAGE. *Lower panel*, Coomassie Brilliant Blue-stained gel of samples of wild type GST-HsMis13 plus Aurora B (GST-HsMis13) and double mutant S100A/S109A GST-HsMis13 plus Aurora B (GST-HsMis13$^{S100A/S109A}$). Note that roughly equivalent amounts of GST-HsMis13 protein were present in the two reactions. *Upper panel*, the same gel was dried and subsequently incubated with x-ray film. Note that there was dramatic incorporation of ^{32}P into wild type but little into the double mutant, HsMis13 proteins. *D*, quantification of ^{32}P incorporation into HsMis13 protein by Aurora B. The phosphorylation reaction was done as described as *C*. The ^{32}P incorporation into HsMis13 proteins was quantified by a PhosphorImager. The ^{32}P incorporation into wild type HsMis13 and non-phosphorylatable HsMis13$^{S100A/S109A}$ was normalized to their protein levels and expressed as a percentage of wild type. Values represent the means ± S.E. of three different experiments. *E*, HsMis13 is a cognate substrates of Aurora B *in vivo*. Extracts of nocodazole-synchronized mitotic HeLa cells were immunoprecipitated using an anti-HsMis13 antibody. Immunoprecipitates were then fractionated by SDS-PAGE followed by transferring onto a nitrocellulose membrane. Immunoblotting of HsMis13 immunoprecipitated protein (*top panel*, *Mis13*) and serine phosphorylation of HsMis13 (*lower panel*, *Phospho-Mis13*). Note that the Aurora B inhibitor VX-680 treatment markedly suppressed HsMis13 phosphorylation but not the protein accumulation. *F*, Ser-100 and Ser-109 of HsMis13 are phosphorylated in mitosis. Extracts from mitotic HeLa cells transiently transfected to express GFP-HsMis13 and GFP-HsMis13^{AA} (both Ser-100 and Ser-109 were mutated to Ala) were incubated with an anti-GFP antibody and immunoprecipitates were resolved by SDS-PAGE followed by transferring onto a nitrocellulose membrane. The membrane was first probed for GFP-HsMis13 (*upper panel*) followed by detection of phosphoserine (*lower panel*). *Lane 1*, GFP-HsMis13 immunoprecipitates. *Lane 2*, GFP-HsMis13^{AA} immunoprecipitates. Note that GFP-HsMis13^{AA} was not detected by phosphoserine antibody.

If HsMis13 is a cognate binding partner of Aurora B, they should co-distribute to kinetochore of mitotic cells. To this end we performed an immunocytochemical staining in which an anti-HsMis13 rabbit antibody and an anti-Aurora B mouse antibody were employed to mark their kinetochore distribution. As shown in Fig. 1*B*, Aurora B displayed a typical inner kinetochore distribution from prophase to metaphase in HeLa cells (*arrows*; *c*, *g*, and *k*), whereas HsMis13 exhibited a typical pair of separated kinetochore spots (arrowheads; *a*, *e*, and *i*). The merged image confirmed their relative co-distribution at the centromere (*arrow*; *d*, *h*, and *l*).

HsMis13 Is a Novel Substrate of Aurora B—Because HsMis13 binds to Aurora B *in vivo*, we sought to test if HsMis13 is a substrate of Aurora B. Our computational analysis suggests that Ser-100 and Ser-109 are potential substrates of Aurora B (19), which are conserved among vertebrate HsMis13 proteins. To test whether Ser-100 and Ser-109 are substrates of Aurora B, we performed *in vitro* phosphorylation on recom-

binant GST-HsMis13 fusion proteins, including both wild type HsMis13 and non-phosphorylatable HsMis13 mutants in which Ser-100 and Ser-109 were both replaced by alanine ($HsMis13^{S100A/S109A}$). Both GST fusion proteins, wild type and mutant $HsMis13^{S100A/S109A}$, migrated to about the predicted 68 kDa as shown in Fig. 1*C*. Incubation of the fusion proteins with [^{32}P]ATP and His-Aurora B resulted in the incorporation of ^{32}P into wild type but not $HsMis13^{S100A/S109A}$ mutant (Fig. 1*C*, *upper panel*). This Aurora B-mediated phosphorylation is specific, as incubation of HsMis13 with [^{32}P]ATP in the absence of Aurora B resulted in no detectable incorporation of radioactivity into the wild type protein (data not shown). The specific incorporation of ^{32}P into wild type protein *versus* non-phosphorylatable mutant was quantified and shown in Fig. 1*D*, which show that only background level ^{32}P was incorporated into non-phosphorylatable HsMis13 protein in the presence of active Aurora B kinase. Thus, we conclude that both Ser-100 and Ser-109 on HsMis13 are substrates of Aurora B *in vitro*.

If HsMis13 is a substrate of Aurora B *in vivo*, suppression of Aurora B kinase activity using chemical inhibitors, such as VX-680 (20), would alter endogenous HsMis13 phosphorylation. Indeed, suppression of Aurora B using VX-680 reduced serine phosphorylation of HsMis13 immunopurified from mitotic HeLa cells (Fig. 1*E*), suggesting that HsMis13 is a cognate substrate of Aurora B in mitosis.

To validate if Ser-100 and Ser-109 are Aurora B substrates *in vivo*, we conducted an anti-GFP immunoprecipitation of nocodazole-arrested mitotic cell lysates from HeLa cells transiently transfected to express GFP-HsMis13 and GFP-$HsMis13^{S100A/S109A}$ proteins. Importantly, GFP-HsMis13 protein but not GFP- $HsMis13^{S100A/S109A}$ mutant protein contains serine phosphorylation judging by anti-phosphoserine Western blotting analysis (Fig. 1*F*). Thus, we conclude that Ser-100 and Ser-109 of HsMis13 are endogenous substrates of Aurora B in mitotic cells.

Aurora B Kinase Activity Controls the Kinetochore Localization of HsMis13—To investigate the possible influence of Aurora B on the localization of HsMis13 to the kinetochore, we introduced siRNA oligonucleotide duplexes to Aurora B by transfection into HeLa cells. Trial experiments revealed that treatment of HeLa cells with 150 nM siRNA for 36 h produced an optimal suppression of the target protein. As shown in Fig. 2*A*, Western blot with an anti-Aurora B antibody revealed that the siRNA oligonucleotide caused remarkable suppression of Aurora B protein levels at 36 h. This suppression is relatively specific as it did not alter the levels of other proteins such as tubulin and HsMis13.

Next, we examined the effect of repressing Aurora B on the localization of HsMis13 to the kinetochore. HeLa cells were subcultured on coverslips in 24-well plates and transfected with siRNA. In control scramble siRNA-transfected cultures, Aurora B and HsMis13 were co-distributed to the kinetochore of prometaphase and metaphase cells (Fig. 2*B*, *a*–*h*). In cells in which Aurora B had been suppressed, the levels of kinetochore-bound HsMis13 appeared reduced (Fig. 2*B*; *a′*–*h′*). Quantification of normalized pixel intensities shows that, when Aurora B was reduced to less than 11% that of its control value, HsMis13 levels were reduced to ~29%, indicating that Aurora B is required for efficient kinetochore localization of HsMis13 (Fig. 2*D*).

Because Aurora B and HsMis13 form a stable complex, failure of HsMis13 localization to the kinetochore could be mediated by their physical interactions. To assess whether Aurora B kinase activity rather than its physical interaction with HsMis13 controls the kinetochore localization of HsMis13, we sought to use Aurora B inhibitor VX-680 and hesperadin to suppress Aurora kinase activity and then assess the effect of Aurora B inhibition on the localization of HsMis13 to the kinetochore. As shown in Fig. 2*C* (*c′*), 1 μM VX-680 almost completely suppressed histone 3 phosphorylation on Ser-10, an endogenous substrate of Aurora B, consistent with the literature (20). Examination of the same cells treated with VX-680 revealed that HsMis13 localization to the kinetochore was minimized (Fig. 2*C*, *a′*). Quantification of normalized pixel intensities shows that, when Aurora B activity was reduced to less than 10% that of its control value as judged by histone Ser-10 phosphorylation, HsMis13 levels were reduced to ~31% (Fig. 2*D*). Experimentation with another Aurora B kinase inhibitor hesperadin gave essentially the same outcome (data not shown). Thus, we conclude that Aurora B kinase activity controls the localization of HsMis13 to the kinetochore.

HsMis13 Exhibits a Cell Cycle-dependent Distribution to Kinetochore—The cell cycle-regulated spatiotemporal dynamics of Aurora B propelled us to examine the distribution profile of HsMis13 in mitotic cells. Western blotting analyses of synchronized HeLa cell lysates show that the HsMis13 protein expression level is relatively constant during cell cycle, whereas CENP-E and cyclin B levels exhibit a typical cyclic wave (Fig. 3*A*). We next examined the spatiotemporal distribution of HsMis13 in HeLa cells. The ACA immunofluorescence study shows a typical labeling of centromere in interphase nucleus and kinetochore of mitotic cells (Fig. 3*B*, *green*). However, HsMis13 began to appear on the kinetochore marked by ACA staining in prophase and remains associated with kinetochore until anaphase B. In telophase, ACA staining remains associated with kinetochore, whereas HsMis13 is no longer associated with kinetochore (Fig. 3*B*, *g*), suggesting that HsMis13 is assembled onto the centromere during interphase and released from centromere at telophase. To test if HsMis13 localization to kinetochore is correlated with its phosphorylation by Aurora B, we isolated the HsMis13 from prophase and telophase lysates from thymidine synchronized and released HeLa cells. Consistent with our hypothesis, the HsMis13 isolated from prophase, but not telophase cells, contains a phosphoserine epitope (Fig. 3*C*). The lack of Ser-10 phosphorylation of histone 3 indicates that Aurora B activity is minimized at the kinetochore of telophase cells (Fig. 3*C*; *left*). Thus, we reason that cell cycle-regulated association of HsMis13 with the kinetochore is a function of Aurora B phosphorylation.

Aurora B-mediated Phosphorylation Determines HsMis13 Association with Kinetochore—To directly examine the role of Aurora B-mediated phosphorylation in HsMis13 localization to the kinetochore, we generated non-phosphorylatable and phosphomimetic HsMis13 mutations and transiently transfected HeLa cells with GFP-tagged mutant plasmids. Western

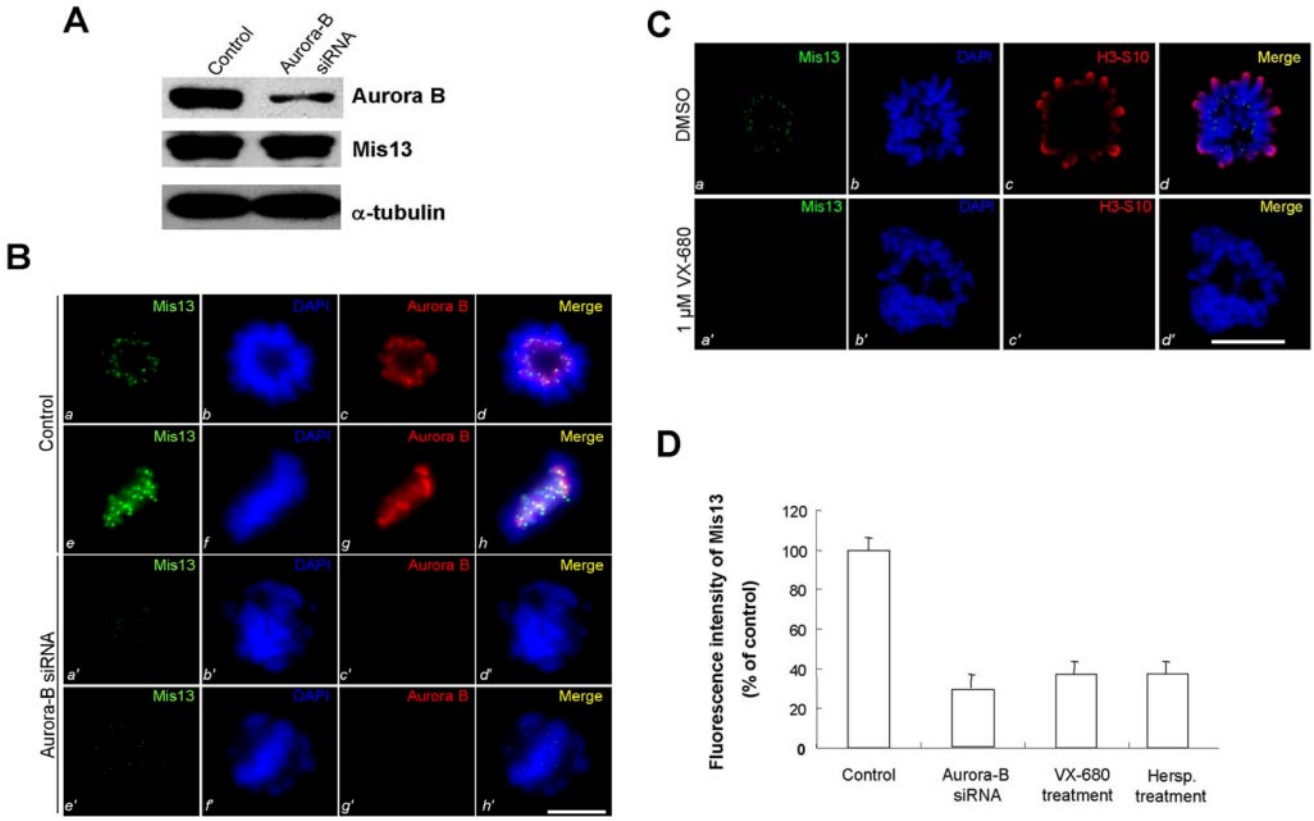

FIGURE 2. **Aurora B kinase determines the kinetochore localization of HsMis13.** *A*, Aurora B siRNA suppressed the Aurora B protein accumulation. Aliquots of HeLa cells were transfected with Aurora B siRNA and scramble control as described under "Materials and Methods." Cells were then harvested for SDS-PAGE and subsequent Western blotting analyses of the efficiency on suppression of Aurora B protein (*upper panel*) and specificity of this siRNA-mediated Aurora B depletion (*middle* and *lower panel*). *B*, suppression of Aurora B prevented kinetochore distribution of HsMis13. Aliquots of HeLa cells were transfected with Aurora B siRNA and scramble control as described under "Materials and Methods." Cells were then harvested for immunofluorescence staining of HsMis13 (*green*), Aurora B (*red*), and DNA (*blue*). HsMis13 co-distributes with Aurora B to the kinetochore of scramble-transfected cells (*d* and *h*). Suppression of Aurora B by siRNA eliminates the kinetochore localization of Mis13 (*a′* and *e′*). Note that Aurora B siRNA-treated cells displayed a typical chromosome congressional defect in mitotic cells. The *scale bar* represents 10 μm. *C*, inhibition of Aurora B kinase activity eliminated kinetochore localization of HsMis13. Aliquots of HeLa cells were treated with an Aurora B inhibitor VX-680 and DMSO as described under "Materials and Methods." Cells were then harvested for immunofluorescence staining of HsMis13 (*green*), phospho-Ser-10-histone 3 (*red*), and DNA (*blue*). Phospho-Ser-10-histone labeling distributes to the mitotic chromosome arms in DMSO-treated cells (*c*). Inhibition of Aurora B by 1 μM VX-680 suppressed phosphorylation of Ser-10 of histone 3 and eliminated the kinetochore localization of HsMis13 (*a′*). The *scale bar* represents 10 μm. *D*, quantitation of HsMis13 levels at kinetochores of control, Aurora B siRNA-treated, and VX-680-treated and hesperadin (*Hersp.*)-treated cells. The pixel intensities of HsMis13 normalized to the ACA signal in control, and Aurora B-repressed and Aurora B kinase activity-inhibited cells were measured. Values represent the means ± S.E. of at least 100 kinetochores in 10 different cells.

blotting analysis carried out using transfected HeLa cell preparations showed that the exogenously expressed GFP-HsMis13 protein was about twice the level of endogenous HsMis13 (Fig. 4*A*). Given the transfection efficiency of 55~60%, the actual expression level of GFP-HsMis13 in positively transfected cells is about 3-fold higher than that of endogenous protein.

The subcellular localization of the exogenously expressed GFP-HsMis13 constructs was compared with that of HsMis12 by fluorescence microscopy. The transfected cells were triple-stained for GFP-HsMis13 using a monoclonal GFP antibody (*green*) and counterstained for HsMis12 (*red*) and DNA (*blue*). Fig. 4*B* shows the confocal image from wild type GFP-HsMis13-transfected cells. Similar to what has been noted in endogenous HsMis13 distribution, GFP-tagged HsMis13 distributes to the kinetochore of prophase cells (Fig. 4*B*, *b*) and is superimposed onto that of HsMis12 when the two channels are merged (Fig. 4*B*, *d*).

Our examination of GFP- HsMis13$^{S100A/S109A}$-transfected cells revealed that non-phosphorylatable HsMis13 fails to localize to the kinetochore, whereas the kinetochore distribution of HsMis12 remains (Fig. 4*C*). As predicted, phosphomimetic HsMis13 is localized to the kinetochore in a pattern similar to that of wild type HsMis13 (Fig. 4*D*). Thus, we conclude that Aurora B-mediated phosphorylation of HsMis13 at Ser-100 and Ser-109 controls the localization of HsMis13 to the kinetochore.

Aurora B-mediated Phosphorylation of HsMis13 Is Essential for Kinetochore Assembly—HsMis13 is an important component of HsMis12 centromere core complex and is essential for outer kinetochore protein complex assembly (*e.g.* Refs. 11–13). However, it has remained elusive as to how the HsMis12 complex assembly is regulated and whether this determines the outer kinetochore protein complex assembly. To investigate the possible influence of HsMis13 on the localization of outer kinetochore protein complex assembly, we introduced siRNA oligonucleotide duplexes into HsMis13 by transfection into HeLa cells. As shown in Fig. 5*A*, Western blot with an anti-HsMis13 antibody revealed that the siRNA oligonucleotide caused remarkable suppression of HsMis13 protein level at

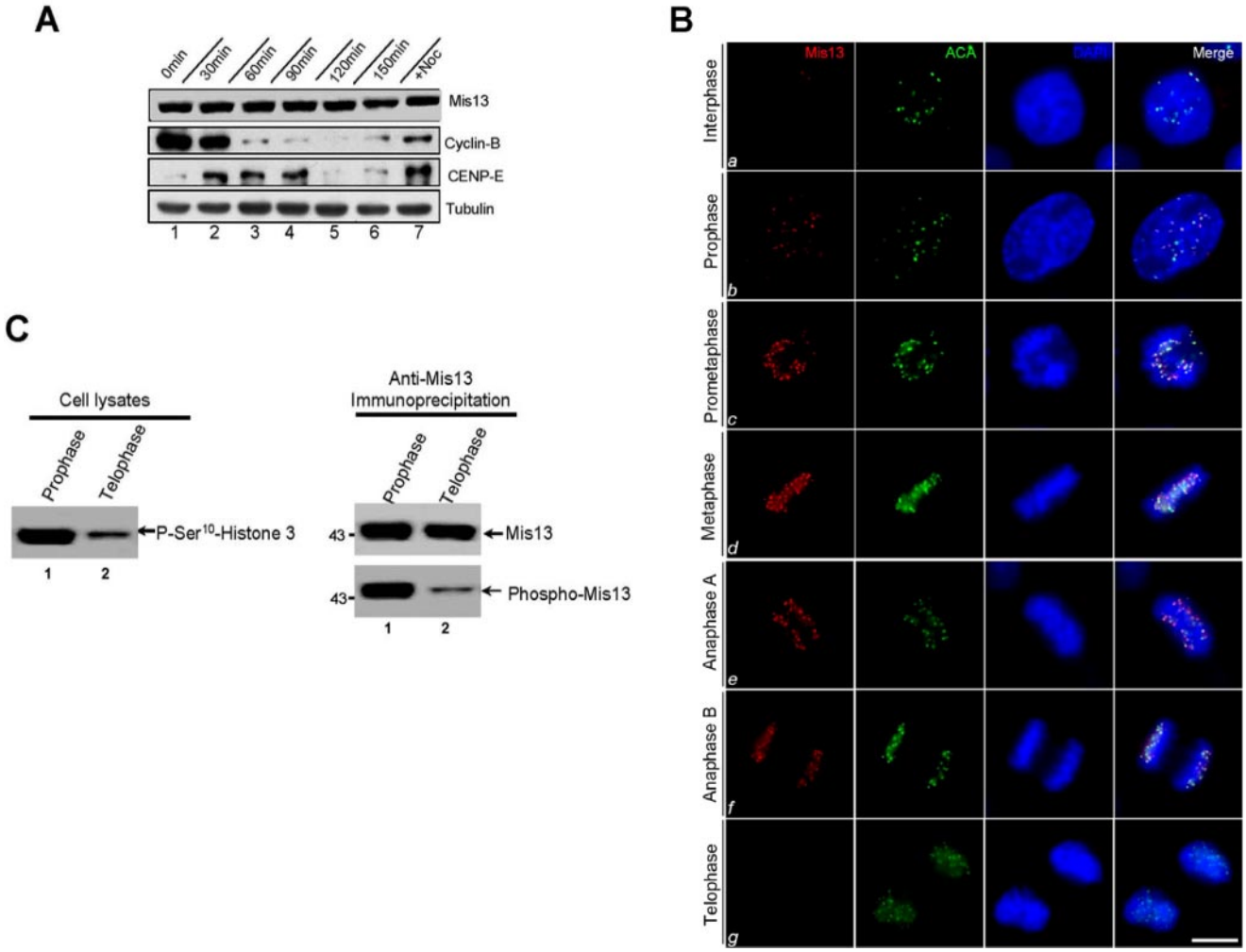

FIGURE 3. **Characterization of the spatiotemporal pattern of HsMis13 phosphorylation and distribution.** *A*, HsMis13 protein levels are relatively constant during cell cycle. Aliquots of HeLa cells were collected from double thymidine-synchronized cells as described under "Materials and Methods" for SDS-PAGE and subsequent Western blotting analyses of the protein levels of HsMis13 (*upper panel*), cyclin B, CENP-E (*middle panels*), and tubulin (*lower panel*). *Noc*, nocodazole. *B*, HsMis13 distributes to the kinetochore at late interphase and departs from kinetochore at the telophase. Asynchronized mitotic HeLa cells were fixed for immunofluorescence staining of HsMis13 (*red*), ACA (*green*), and DNA (*blue*). HsMis13 starts to co-distribute with centromere marker ACA to the kinetochore of late interphase cells (*a*) and becomes overlapped with ACA staining beginning in prophase (*b*) and remaining until late anaphase (*f*). HsMis13 departs from kinetochore in the telophase (*g*). The scale bar represents 10 μm. *C*, phosphorylation of HsMis13 is temporally controlled in mitosis. Aliquots of synchronized HeLa cells were from prophase and telophase as described under "Materials and Methods." Cells were lysed followed by immunoprecipitation with an anti-HsMis13 antibody. Although equal HsMis13 proteins were isolated from prophase and telophase cells (*right upper panel*), little HsMis13 from telophase cells contains phosphoserine epitopes (*right lower panel*; *lane 2*). Probing with an anti-phospho (*P*)-Ser-10 antibody confirmed less abundance of phospho-H3 from telophase cells (*left panel*; *lane 2*).

48 h. This suppression is relatively specific as it did not alter the levels of other proteins such as Aurora B, CENP-E, and CENP-F, etc.

Because HsMis13 and HsMis12 form a stable and evolutionarily conserved kinetochore core complex, we next examined the effect of repressing HsMis13 on the localization of CENP-E and CENP-F to the kinetochore. HeLa cells were subcultured on coverslips in 24-well plates and transfected with siRNA. In control cultures, HsMis13 localized with ACA at the prometaphase kinetochores (Fig. 5*B*, *Control*). In cells in which HsMis13 had been suppressed, the levels of kinetochore-bound CENP-E appeared reduced (Fig. 5*B*, *e′*–*h′*). Quantification of normalized pixel intensities shows that, when HsMis13 was reduced to less than 10% that of its control value, CENP-E level were reduced to ~37%, indicating that HsMis13 is required for efficient kinetochore localization of CENP-E, consistent with previous studies (14). However, in these HsMis13-repressed cells, the levels of ACA and CENP-F detectable at kinetochores appeared largely unaffected (Fig. 5*B*, *c′* and *k′*). Quantification of normalized pixel intensities shows that when HsMis13 was reduced to less than 10% that of its control value, CENP-F levels were modestly reduced to ~69% that of its control, suggesting that CENP-F location to kinetochore is also dependent on HsMis13 but to a less degree.

In cells in which HsMis13 had been suppressed, the levels of kinetochore-bound HsHec1 and HsNuf2 were also reduced. Quantification of normalized pixel intensities shows that, when HsMis13 was reduced to less than 10% that of its control value, HsNuf2 levels were reduced to ~21%, whereas Hec1 levels were reduced to ~23% (Fig. 5*C*), indicating that HsMis13 is required for efficient kinetochore localization of Ndc80 complex,

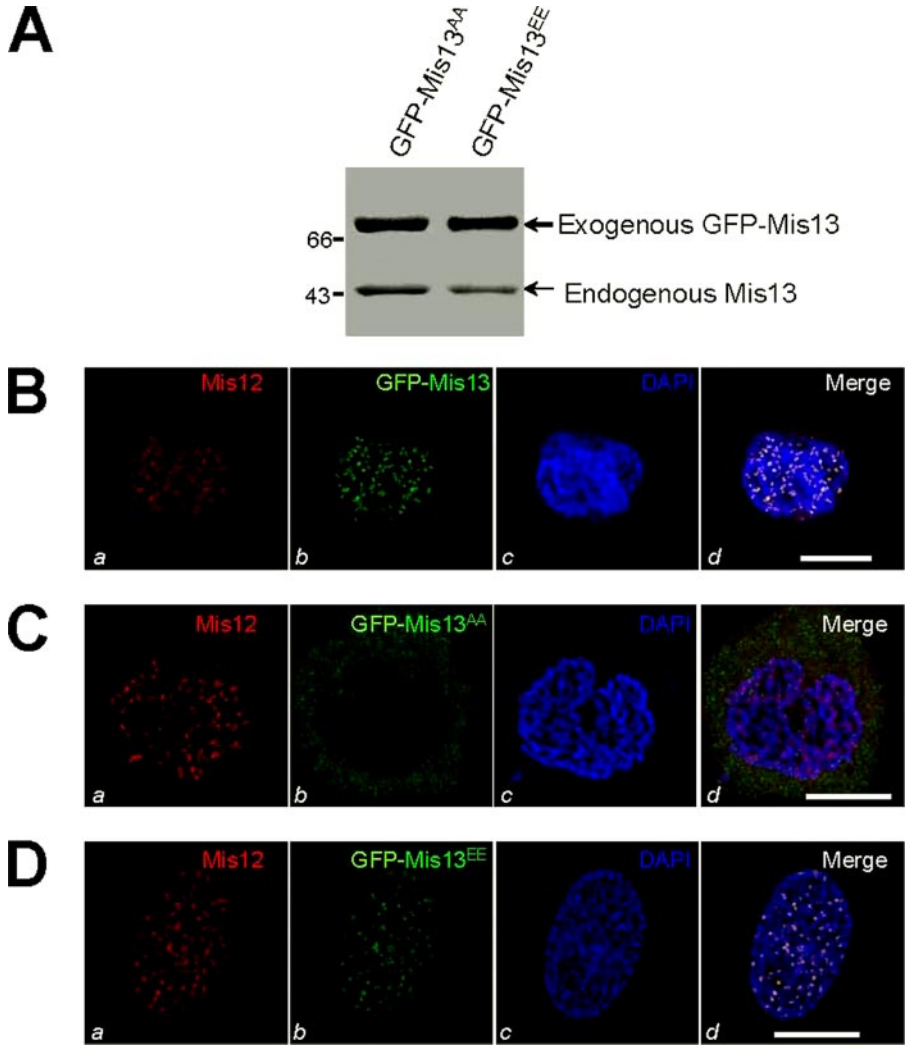

FIGURE 4. **Phosphorylation of HsMis13 by Aurora B is essential for its kinetochore localization.** *A*, expression of exogenous GFP-HsMis13 in HeLa cells. Samples from both phospho-mimicking and non-phosphorylatable-HsMis13-transfected HeLa cells were prepared and separated on SDS-PAGE, blotted to nitrocellulose, and probed by an anti-HsMis13 antibody. Note that the HsMis13 antibody recognizes both endogenous and exogenously expressed GFP-HsMis13 proteins. *B*, exogenously expressed GFP-HsMis13 protein behaves like endogenous HsMis13. HeLa cells were transiently transfected to express GFP-HsMis13 followed by preparation for immunofluorescence staining of HsMis12 (*red*), GFP-HsMis13 (*green*), and DNA (*blue*). GFP-HsMis13 co-distributes with HsMis12 to the kinetochore of mitotic cells (*d*). The *scale bar* represents 10 μm. *C*, non-phosphorylatable GFP- HsMis13$^{S100A/S109A}$ protein failed to localize at the kinetochore. HeLa cells were transiently transfected to express non-phosphorylatable GFP-HsMis13^{AA} followed by preparation for immunofluorescence staining of HsMis12 (*red*), GFP-HsMis13 (*green*), and DNA (*blue*). GFP-HsMis13 ^{AA} failed to distribute with HsMis12 to the kinetochore of mitotic cells (*d*). The *scale bar* represents 10 μm. *D*, phospho-mimicking GFP-HsMis13$^{S100E/S109E}$ protein localizes at the kinetochore. HeLa cells were transiently transfected to express phosphor-mimicking GFP-HsMis13^{EE} followed by preparation for immunofluorescence staining of HsMis12 (*red*), GFP-HsMis13^{EE} (*green*), and DNA (*blue*). GFP-HsMis13^{EE} distributes with HsMis12 to the kinetochore of mitotic cells (*d*). The *scale bar* represents 10 μm.

consistent with the requirement of HsMis12 complex for faithful assembly of Ndc80 complex to outer kinetochore (*e.g.* Ref. 13).

We then examined the effect of Aurora B-mediated phosphorylation of HsMis13 in kinetochore localization of CENP-E. Previous studies show that Aurora B kinase activity controls the assembly of CENP-E to the kinetochore (*e.g.* Refs. 21 and 22). However, it is unclear how Aurora B signaling pathway controls CENP-E localization. If Aurora B-mediated phosphorylation of HsMis13 is essential for kinetochore assembly, expression of phosphomimetic mutant HsMis13 should restore the localization of CENP-E to kinetochore in the absence of Aurora B kinase activity. To test this hypothesis we transfected HeLa cells with wild type and phosphomimetic mutant HsMis13 plasmids followed by treatment of VX-680 to inhibit Aurora B kinase activity.

Consistent with what was observed for endogenous HsMis13 distribution in VX-680-treated cells (Fig. 2*C*, *a*′), GFP-HsMis13 failed to localize to the kinetochore in the presence of Aurora B inhibition (Fig. 5*D*, *b*) whereas HsMis12 remains kinetochore-associated (Fig. 5*D*, *a*). As predicted, the phosphomimetic mutant HsMis13 co-distributes with HsMis12 to the kinetochore in the presence of VX-680 (data not shown), confirming the role of Aurora B-mediated phosphorylation in the control of HsMis13 assembly to the kinetochore.

We next examined whether phosphomimetic mutant HsMis13 can restore CENP-E localization to the kinetochore in the presence of Aurora inhibition. Consistent with our prediction, CENP-E co-distributes with phosphomimetic HsMis13$^{S100E/S109E}$ mutant to kinetochore in the presence of VX-680 (Fig. 5*E*, *a*), whereas little CENP-E appears localized to the kinetochore in GFP-HsMis13-expressing cells in the presence of VX-680 (quantitative analyses in Fig. 5*F*).

As shown in Fig. 5*F*, *open bar*, quantification of normalized pixel intensities shows that the kinetochore-bound CENP-E level in the phosphomimetic HsMis13$^{S100E/S109E}$-expressing cells, is increased from ~27 to ~83% that of its control value (in the absence of VX-680). Thus, we conclude that Aurora B-mediated phosphorylation of HsMis13 is required for the kinetochore localization of CENP-E.

Our recent study demonstrates that Nuf2 interacts with and specifies CENP-E localization to the kinetochore (24). Because CENP-E localization to kinetochore is a function of HsMis13 phosphorylation, we hypothesize that assembly of Nuf2 to the kinetochore is also a function of HsMis13 phosphorylation. As predicted, our quantification shows that the assembly of Nuf2 to the kinetochore in the phosphomimetic HsMis13$^{S100E/S109E}$-expressing cells is also increased (from ~21 to ~67% that of its control value; Fig. 5*F*, *blue bar*), consistent with the fact that Nuf2 mediates CENP-E localization to the kinetochore.

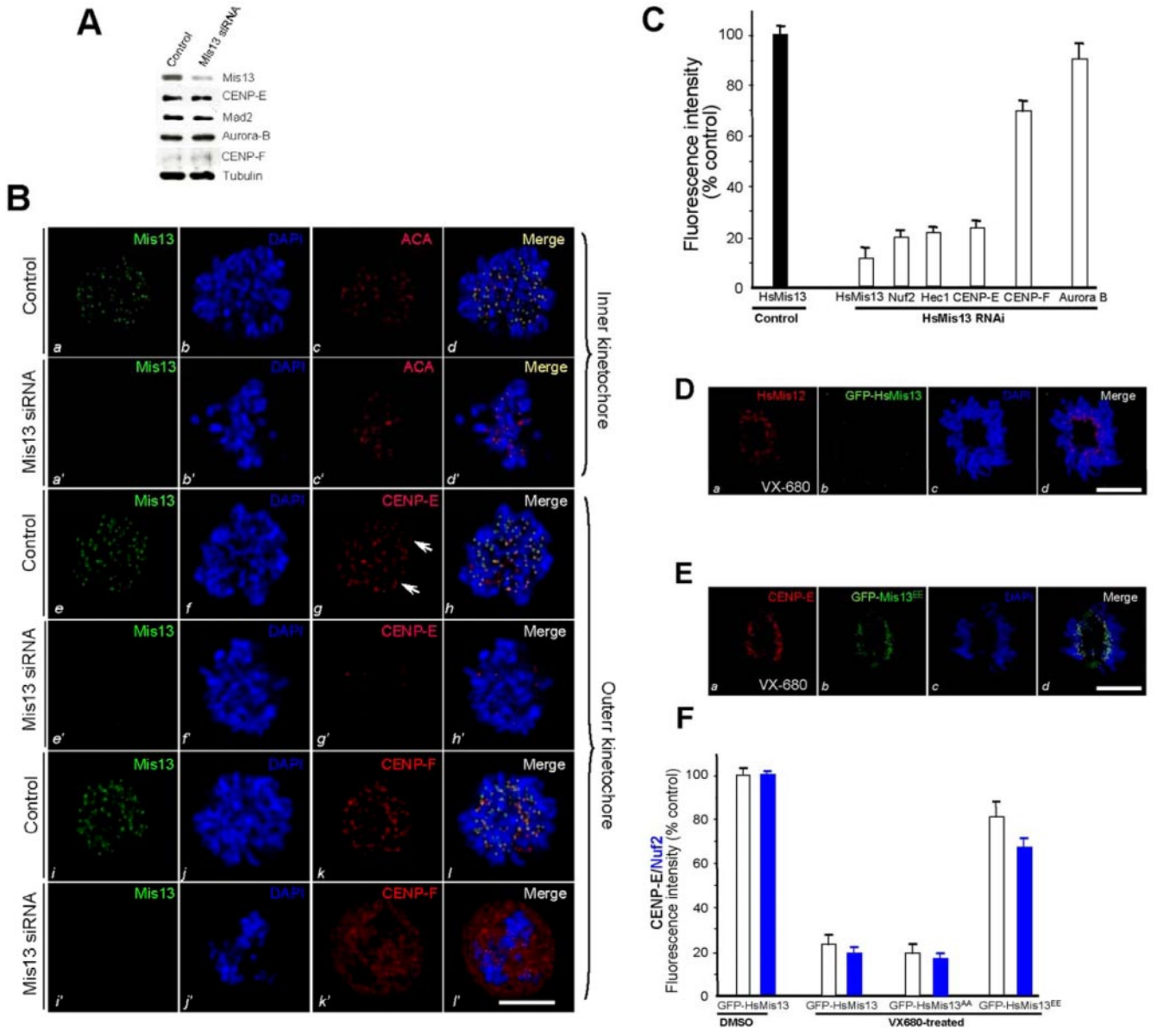

FIGURE 5. **Phosphorylation of HsMis13 is essential for faithful assembly of kinetochore.** *A*, HsMis13 siRNA suppressed the HsMis13 protein accumulation. Aliquots of HeLa cells were transfected with HsMis13 siRNA and scramble control as described under "Materials and Methods." Cells were then harvested for SDS-PAGE and subsequent Western blotting analyses of the efficiency on suppression of HsMis13 protein (*upper panel*) and specificity of this siRNA-mediated HsMis13 depletion by assessing the protein levels of other kinetochore proteins such as Aurora B, CENP-E, CENP-F, and MAD2 (*all lower panels*). *B*, suppression of HsMis13 prevents assembly of CENP-E and CENP-F to the kinetochore. HeLa cells were transfected with HsMis13 siRNA oligonucleotide and control oligonucleotide for 48 h followed by fixation and indirect immunofluorescence staining. This set of optical images was collected from HeLa cells stained for HsMis13 (*green*), ACA (*red*, *c* and *c′*), CENP-E (*red*, *g* and *g′*), CENP-F (*red*, *k* and *k′*), and DNA (*blue*), respectively. As shown in *g*, CENP-E protein is associated with kinetochore as resolved *double dots* in scramble control cells (*arrows*). However, virtually undetectable staining of CENP-E can be seen in HsMis13-depleted cells (*g′*), whereas kinetochore-associated CENP-F and ACA signals were not altered by HsMis13 suppression (*c′* and *k′*). The *scale bar* represents 10 μm. *C*, quantitation of CENP-E, CENP-F, Nuf2, Hec1, and Aurora B levels at kinetochores of control and siRNA-treated cells. The pixel intensities of HsMis13, Nuf2, CENP-E, CENP-F, Aurora B, and Hec1 (normalized to the ACA signal) in control (*closed bar*) and HsMis13-repressed (*open bars;* HsMis13 RNAi) cells were measured. Values represent the means ± S.E. of at least 100 kinetochores in 10 different cells. *D*, inhibition of Aurora B prevented kinetochore distribution of GFP-HsMis13. HeLa cells were transiently transfected to express GFP-HsMis13 followed by treatment of VX-680 as described under "Materials and Methods." Cells were then harvested for immunofluorescence staining of GFP-HsMis13 (*green*), HsMis12 (*red*), and DNA (*blue*). Inhibition of Aurora B by VX-680 eliminated the kinetochore localization of HsMis13 (*b*). The *scale bar* represents 10 μm. *E*, phospho-mimicking GFP-HsMis13^{EE} restored the kinetochore localization of CENP-E at the kinetochore. HeLa cells were transiently transfected to express phospho-mimicking GFP-HsMis13^{EE} followed by treatment of VX-680 as described under "Materials and Methods." Cells were then harvested for immunofluorescence staining of GFP-HsMis13^{EE} (*green*), CENP-E (*red*), and DNA (*blue*). Localization of HsMis13 restored the kinetochore association of CENP-E in the presence of VX-680 (*a* and *b*). The scale bar represents 10 μm. *F*, quantitation of CENP-E and Nuf2 levels at kinetochores of GFP-HsMis13 expressing cells in the presence of Aurora B kinase inhibitor. The pixel intensities of CENP-E levels (normalized to the ACA signal) in control GFP-HsMis13-expressing cells (*open bars*) and GFP-HsMis13-expressing and X-680-treated (*open bars*) cells were measured. The levels of Nuf2 were also measured in the aforementioned conditions (*blue bars*). Values represent the means ± S.E. of at least 100 kinetochores in 10 different cells.

Phosphorylation of HsMis13 Is Essential for Assembly a Stable Microtubule-Kinetochore Attachment—Previous studies have established that CENP-E and the HsNUF2·HEC1 complex are essential for stabilizing microtubule-kinetochore attachments (*e.g.* Refs. 14 and 18). The distance between the sister kinetochores marked by ACA has been used as an accurate reporter

A

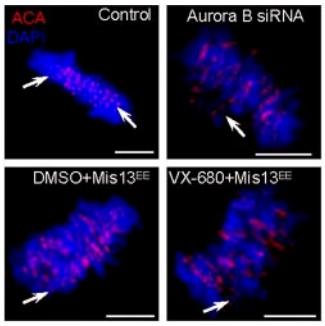

B

Treatment	ACA Distance (μm)
Control	1.69±0.14
Aurora B SiRNA	1.27±0.11
GFP-HsMis13^{EE}+DMSO	1.67±0.17
GFP-HsMis13^{EE}+VX-680	1.53±0.17

*Measured 100 kinetochores from >10 cells of each treatments

FIGURE 6. **Inhibition of Aurora B-mediated phosphorylation of HsMis13 releases the tension across sister kinetochore.** *A*, immunofluorescence assay of control siRNA-treated cells, Aurora B siRNA-treated cells, GFP-HsMis13^{EE}-expressing cells, and GFP-HsMis13^{EE}-expressing and VX-680-treated cells. *B*, quantitation of sister kinetochore distance marked by ACA staining. Kinetochore distance is measured between kinetochores that are marked by ACA staining and localized in the same focal plane as described under "Materials and Methods." Each value from treated samples was calculated from >100 kinetochores selected from at least 10 different cells. *DMSO*, dimethyl sulfoxide.

for judging the tension developed across the kinetochore pair (*e.g.* Ref. 18). In this case shortened distance often reflects aberrant microtubule attachment to the kinetochore, in which less tension is developed across the sister kinetochore. To test the functional activity of microtubule capturing in the cells suppressing Aurora B but expressing phosphomimetic HsMis13$^{S100E/S109E}$ mutant, we measured this distance in 200 kinetochore pairs in which both kinetochores were in the same focal plane in both VX-680-treated cells and control cells (Fig. 6*B*).

As shown in Fig. 6*A*, suppression of Aurora B results in errors in chromosome alignment at the equator, which is consistent with previous reports (*e.g.* Refs. 21 and 23). Control kinetochores exhibited a separation of 1.69 ± 0.14 μm, whereas the mean distance between kinetochores was 1.27 ± 0.11 μm in Aurora B-suppressed cells. Significantly, expression of phosphomimetic HsMis13$^{S100E/S109E}$ mutant increases inter-kinetochore distance (1.53 ± 0.17 μm) in the presence of VX-680. Withdrawal of VX-680 from HsMis13$^{S100E/S109E}$-expressing cells did not significantly extend the inter-kinetochore distance (1.67 ± 0.17 μm). Thus, we conclude that phosphorylation of HsMis13 facilitates the assembly of outer kinetochore which is essential for stable microtubule-kinetochore attachment.

DISCUSSION

The Mis12 Complex Is Composed of Four Proteins: Mis12, Mis13, Mis14, and Mis15. This complex is an essential kinetochore core component highly conserved across species, with a crucial role in kinetochore assembly and proper chromosome segregation during mitosis (11, 17, 18). Our study revealed an important interaction between Aurora B and HsMis13 which is essential for kinetochore assembly and kinetochore-microtubule association.

Previous studies have established that the localization of the Ndc80 complex is exterior to the inner kinetochore proteins such as the HsMis12 complex (11, 13), and the Ndc80 complex localizes to the interior of CENP-E (*e.g.* Refs. 23 and 24). Although the Ndc80 complex is indispensable for establishing kinetochore-microtubule attachments, the HsMis12 complex is linked to heterchromatin via binding to HP1 (*e.g.* Ref. 11). Thus, the Ndc80 complex is postulated to link microtubule-binding proteins and chromatin-bound centromere core proteins. It has been reported that the main function of the Ndc80 complex is to stabilize the microtubule-kinetochore attachment as cells lacking Nuf2 or Hec1 often carry unstable spindle microtubules (23). Our recent finding of CENP-E-Nuf2 interaction provides a novel link between spindle microtubules and the kinetochore core complex via mitotic kinesin CENP-E (24). Consistent with this multiprotein complex architecture, suppression of any component of HsMis12 diminishes the association of CENP-E with the kinetochore (*e.g.* Ref. 13 and this study). It would be of great interest to delineate the precise molecular interaction underlying the HsMis12-Ndc80-CENP-E subcomplex assembly *in vitro* and examine how perturbation of such an interaction alters the plasticity of kinetochore assembly and chromosome segregation by a combination of nanometer-resolution distribution of single molecules with photoactivable fluorescent proteins in living dividing cells (25).

The interaction between spindle microtubules and kinetochore is central to chromosome segregation and stability in mitosis. The four-layer kinetochore ultrastructure is reflected by a stepwise assembly of kinetochore components from the chromatin to the outmost fibrous corona. After breakdown of the nuclear envelope, astral microtubules emanate from centrioles and pass though gaps in the envelope coming in close proximity to newly condensing chromosomes. Using immunoelectron microscopy, CENP-E is found at developing kinetochores adjacent to microtubules at this early stage of mitosis (11). CENP-E is located at the outer kinetochore surface during chromosome bi-orientation, although the kinetochore remains morphologically immature. Despite the ultra-resolution analysis of CENP-E molecular dynamics in mitosis and recent identification of Ndc80 as a key structural determinant for CENP-E localization to kinetochore (24), the molecular architect of mammalian kinetochore has remained elusive. Recent studies have established the role of CENP-A as a fundamental determinant of centromere specification (26) and suggested a potential role of Mis12 complex as a potential link between CENP-A complex and kinetochore assembly foci (11, 13). However, it was unclear how the individual subunit of the conserved four-subunit Mis12 complex is assembled onto the centromere. Our finding that Aurora B phosphorylates HsMis13 and such phosphorylation controls HsMis13 assembly to kinetochore suggests that the complex is assembled at the kinetochore as HsMis12 is located to centromere before HsMis13. Interestingly, the localization of HsMis12 to the centromere is independent of Aurora B kinase. It

would be important and necessary to examine whether and how Aurora B regulates the four-subunit complex assembly *in vitro* and *in vivo*.

One interesting phenotype shown in Fig. 5*E* demonstrates that expressing the phosphomimetic HsMis13$^{S100E/S109E}$ mutant in HeLa cells with diminished Aurora B kinase activity restored the kinetochore localization of CENP-E but fails to correct all misaligned chromosomes, indicating that the molecular regulation of their kinetochore components such as Ndc80 and MCAK by Aurora B is essential for faithful chromosome segregation. Besides its critical role in kinetochore assembly, Aurora kinase also governs kinetochore-microtubule interaction by correcting aberrant attachments (27). Consistent with this notion, recent studies show that phosphorylation of Hec1 by Aurora B is essential to orchestrate a dynamic and faithful kinetochore-microtubule association (28). Parallel biochemical reconstitution experiments show that phosphorylation of Hec1 by Aurora B promotes the microtubule dynamics by promoting a weaker Ndc80-microtubule interaction (29). A fundamental characteristic of the kinetochore-spindle microtubule interface is its ability to maintain stable associations, whereas associated microtubules remain dynamic. Such a feature is coordinated by an array of intrinsically low affinity binding sites which are then modulated by mitotic machinery such as Aurora B kinases. Thus, it would be necessary to generate a specific optical reporter to "read" the spatiotemporal activity of Aurora B quantitatively which will enable us to consolidate HsMis13-Ndc80-microtubule interactions into a model for kinetochore choreography in mitosis. A recent study has indeed demonstrated feasibility of using such a reporter to visualize Aurora B kinase gradient in real-time mitosis (30). It would be of great interest to test reversion of Aurora B phosphorylation dictates the liberation of HsMis13 from kinetochore in real-time mitosis using the aforementioned reporter combined with Aurora B inhibitor.

The aberrant Hec1 and Nuf2 targeting in the HsMis13-depleted cell is likely due to a disruption in a direct HsMis12-Ndc80 interaction given the conserved physical interaction between the Mis12 and Ndc80 complexes. Expression of the phosphomimetic HsMis13$^{S100E/S109E}$ mutant in HeLa cells with diminished Aurora B kinase activity restored the kinetochore localization of Hec1 and Nuf2 (~67% that of control; Fig. 5*F*) but fails to correct all misaligned chromosomes. Given the contribution of CENP-H pathway in Ndc80 assembly to the kinetochore (~30%; *e.g.* Ref. 11), it is possible that global inhibition of Aurora B also inhibits the CENP-H pathway, which accounts for the defects in chromosome alignment seen in the phosphomimetic HsMis13$^{S100E/S109E}$-expressing HeLa cells.

Taken together, we propose that phospho-regulation of HsMis13 by Aurora B establishes faithful kinetochore-microtubule attachment by recruiting outer kinetochore proteins and correcting aberrant kinetochore-microtubule attachment errors. It is likely that all of the kinetochore outer plate proteins interact to orchestrate a functional kinetochore during chromosome segregation. The Aurora B-HsMis13 interaction established here is a core of this giant and dynamic complex, which orchestrates kinetochore structure core complex assembly to spindle microtubule attachment in the centromere.

Acknowledgments—We thank members of our groups for insightful discussion during the course of this study. The facilities were supported in part by NIH/NCRR/RCM1 Grant G-12-RR03034.

REFERENCES

1. Cleveland, D. W., Mao, Y., and Sullivan, K. F. (2003) *Cell* **112,** 407–421
2. Musacchio, A., and Salmon, E. D. (2007) *Nat. Rev. Mol. Cell Biol.* **8,** 379–393
3. Ke, Y., Dou, Z., Zhang, J., and Yao, X. (2003) **13,** 69–81
4. Nigg, E. A. (2001) *Nat. Rev. Mol. Cell Biol.* **2,** 21–32
5. Fu, G., Ding, X., Yuan, K., Aikhionbare, F., Yao, J., Cai, X., Jiang, K., and Yao, X. (2007) *Cell Res.* **17,** 608–618
6. Tanaka, T. U. (2005) *Philos. Trans. R. Soc. Lond. B. Biol. Sci.* **360,** 581–589
7. Takahashi, K., Yamada, H., and Yanagida, M. (1994) *Mol. Biol. Cell* **5,** 1145–1158
8. Goshima, G., Saitoh, S., and Yanagida, M. (1999) *Genes Dev.* **13,** 1664–1677
9. Goshima, G., Kuyomitsu, K., Yoda, D., and Yanagida, M. (2003) *J. Cell Biol.* **60,** 25–39
10. Chesseman, I. M., Niessen, A., Anderson, S., Hyndman, F., Yates, J. R., III, Oegema, K., and Desai, A. (2004) *Gene Dev.* **18,** 2255–2268
11. Obuse, C., *et al.* (2004) *Nat. Cell Biol.* **6,** 1135–1141
12. Liu, X., McLeod, I., Anderson, S., Yates, J. R., and He, X. (2005) *EMBO J.* **24,** 2919–2930
13. Kline, S. L., Cheeseman, I. M., Hori, T., Fukagawa, T., and Desai, A. (2006) *J. Cell Biol.* **173,** 9–17
14. He, X., Rines, D. R., Espelin, C. W., and Sorger, P. K. (2001) *Cell* **106,** 195–206
15. Cao, X., Ding, X., Guo, X., Zhou, R., Forte, J. G., Teng, M., and Yao, X. (2005) *J. Biol. Chem.* **280,** 13584–13592
16. Yao, X., Anderson, K., and Cleveland, D. W. (1997) *J. Cell Biol.* **139,** 435–447
17. Yao, X., Abrieu, A., Zheng, Y., Sullivan, K. F., and Cleveland, D. W. (2000) *Nat. Cell Biol.* **2,** 484–491
18. Johnson, V. L., Scott, M. I. F., Holt, S. V., Hussein, D., and Taylor, S. S. (2003) *J. Cell Sci.* **117,** 1577–1589
19. Xue, Y., Zhou, F., Lu, H., Chen, G., and Yao, X. (2005) *Nucleic Acids Res.* **33,** 184–187
20. Harrington, E. A., Bebbington, D., Moore, J., Rasmussen, R. K., Ajose-adeogun, A. O., Nakayama, T., Graham, J. A., Demur, C., Hercend, T., Diu-Hercend, A., Su, M., Grolec, J. M., and Miller, K. M. (2004) *Nat. Med.* **10,** 262–267
21. Murata-Hori, M., and Wang, Y. L. (2002) *Curr. Biol.* **12,** 894–899
22. Ditchfield, C., Johnson, V. L., Tighe, A., Ellston, R., Haworth, C., Johnson, T., Mortlock, A., Keen, N., and Taylor, S. S. (2003) *J. Cell Biol.* **161,** 267–280
23. DeLuca, J. G., Dong, Y., Hergert, P., Strauss, J., Hickey, J. M., Salmon, E. D., and McEwen, B. F. (2005) *Mol. Biol. Cell* **16,** 519–531
24. Liu, D., Ding, X., Du, J., Cai, X., Huang, Y., Ward, T., Shaw, A., Yang, Y., Hu, R., Jin, C., and Yao, X. (2007) *J. Biol. Chem.* **282,** 21415–21424
25. Betzig, E., Patterson, G. H., Sougrat, R., Lindwasser, O. W., Olenych, S., Bonifacino, J. S., Davidson, M. W., Lippincott-Schwartz, J., and Hess, H. F. (2006) *Science* **313,** 1642–1645
26. Jansen, L. E., Black, B. E., Foltz, D. R., and Cleveland, D. W. (2007) *J. Cell Biol.* **176,** 795–805
27. Lampson, M. A., Renduchitala, K., Khodjakov, A., and Kapoor, T. M. (2004) *Nat. Cell Biol.* **6,** 232–237
28. DeLuca, J., Gall, W. E., Ciferri, C., Cimini, D., Musacchio, A., and Salmon, E. D. (2006) *Cell* **127,** 969–982
29. Cheeseman, I. M., Chappie, J. S., Wilson-Kubalek, E. M., and Desai, A. (2006) *Cell* **127,** 983–997
30. Fuller, B. G., Lampson, M. A., Foley, E. A., Rosasco-Nitcher, S., Le, K. M., Tobelmann, P., Brautigan, D. L., Stukenberg, P. T., and Kapoor, T. M. (2008) *Nature* **453,** 1132–1136